Crustal Deformation Caused by the 2016 Kumamoto Earthquake Revealed by GEONET

Satoshi KAWAMOTO, Yohei HIYAMA, Reiko KAI, Fumio SUGA, Kazunori YAMAGUCHI, Tomoaki FURUYA, Satoshi ABE and Naofumi TAKAMATSU

(Published online: 28 December 2016)

Abstract

GNSS observation over the area of the 2016 Kumamoto Earthquake (April 14-16, 2016) reveals coseismic deformations of over 10 centimeters caused by the two large foreshocks and of ~ 1 meter caused by the mainshock as well as a postseismic deformation of up to a few centimeters. Large displacements are concentrated around Futagawa-Hinagu fault zone which is a known active fault in Kyushu Island. Kinematic positioning results imply the two large foreshocks initiated a rupture on the northern part of the Hinagu fault segment, then a rupture neighboring the southern part of the segment. The postseismic deformations that followed seem to be similar to the pattern of coseismic deformation, however, they are widely distributed. The sequence of earthquakes caused significant distortion in the Japanese geodetic datum around the focal area, but GEONET observation enabled a rapid response. Furthermore, it is believed the observation data provided by GEONET will make a significant contribution to understand the fault property along the active fault zone.

1. Introduction

The 2016 Kumamoto Earthquake (*M* 7.3) occurred at 01:25 JST on April 16, 2016, with two large foreshocks (*M* 6.5, *M* 6.4) occurring at 21:26 JST on April 14 and 00:03 JST on April 15, respectively, damaging a wide area around the Kumamoto region, Kyushu Island, Japan. The epicenters of the mainshock and the two foreshocks are located in the Oita-Kumamoto tectonic line (e.g. Saiga et al., 2010), which belongs to a large right-lateral shear zone, an extension of the median tectonic line (MTL) which is running through the central part of Kyushu Island (Matsumoto et al., 2015).

The aftershock distribution and the focal mechanism indicate that the mainshock occurred along the Futagawa fault (Fig. 1; Yagi et al., 2016). In addition, the geodetic measurements including GNSS and InSAR observations indicate the coseismic slip occurred along the Futagawa–Hinagu fault zone with right-lateral slip as well as some of strike slip component (Yarai et al., 2016). Based on the observation results above, the Headquarters for Earthquake Research Promotion (HERP), which is a governmental committee that evaluates earthquake activities in Japan reported that the 2016 Kumamoto Earthquake was mainly caused due to the activity of the Futagawa fault segment (HERP, 2016). In contrast to the mainshock, the finite fault model inversion results for the two foreshocks show pure right-lateral motion along the northern part of the Hinagu fault segment (Kobayashi, 2016; Yarai et al., 2016).

The ground displacements estimated from GNSS observation are very powerful data to constrain the fault parameters including e.g. fault geometry, fault slip, and magnitude. The Geospatial Information Authority of Japan (GSI) is operating the nationwide GNSS network GNSS Earth Observation Network (GEONET), which consists of ~1,300 continuous GNSS-based control stations with a coverage interval of 20–30 km (Yamagiwa et al., 2006). The GEONET data is processed with three kinds of routine analyses: F3 (24-hour session/latency of two weeks), R3 (24-hour session/latency of two days), and Q3 (6-hour session/latency of nine hours; Nakagawa et al., 2009). Since the two foreshocks on April 14 and April 15 occurred consecutively within three hours, the coseismic displacements could not be extracted from the routine analyses separately. However, the GEONET real-time analysis system (REGARD; Kawamoto et al., 2015), which offers 1 Hz kinematic solutions successfully detected coseismic displacements for each earthquake individually.

This paper discusses the crustal deformations caused by the 2016 Kumamoto Earthquake sequence inferred from the GNSS observations by GEONET. The coseismic displacements caused by the two foreshocks are estimated from the kinematic solutions from REGARD system, and are compared with the static offsets extracted from the routine analysis. Then the coseismic displacements caused by the mainshock estimated from the GEONET routine analysis are presented. Furthermore, the significant post-seismic deformations observed around the focal area are shown.

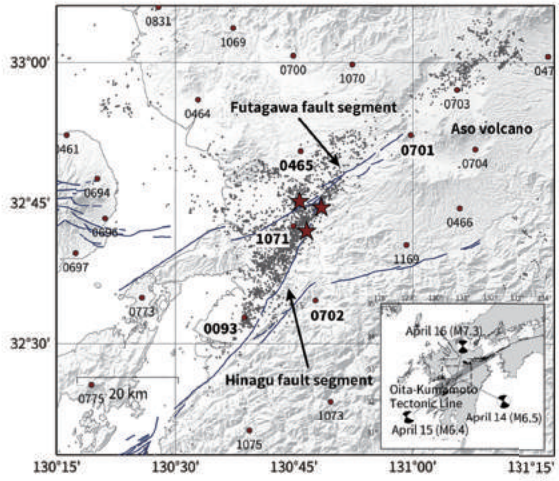

Fig. 1 Station distribution and tectonic setting of the Futagawa–Hinagu fault zone. The red circles indicate the GEONET sites. The red stars and gray dots show the epicenters for the 2016 Kumamoto Earthquake sequence and its aftershocks, respectively. Focal mechanisms are also shown in the inset. Blue lines denote the active fault traces (HERP, 2013).

2. Coseismic Deformations Caused by the Two Large Foreshocks: April 14 Event (*M* 6.5) and April 15 Event (*M* 6.4)

Two days prior to the mainshock, a large foreshock (*M* 6.5) occurred around the junction between the Futagawa fault and Hinagu fault segments, on April 14, 2016 at 21:26 JST. The second large foreshock (*M* 6.4) occurred 5 km south from the first foreshock. Since these two foreshocks occurred in less than three hours, individual coseismic displacements could not be separated by the routine analysis (Kawamoto et al., 2016).

The coseismic displacement field was estimated using the differences between F3 solution before the *M* 6.5 event and Q3 solution after the *M* 6.4 event, relative to the reference site 0388. The displacements include the effects of both the M6.5 and M6.4 events because of the lack of time resolution of the routine analysis. The result shows significant coseismic displacements larger than a few centimeters (Fig. 2). Horizontal displacements of 12 cm and 20 cm with predominantly northern displacements were observed at sites 0465 and 1071 just north of the Hinagu fault segment. On the other hand, a horizontal displacement of 5 cm to the southern direction was observed at site 0702 south of the fault. This deformation pattern implies right-lateral slip along the Hinagu fault segment. However, individual contribution of each foreshock was not clear from this result.

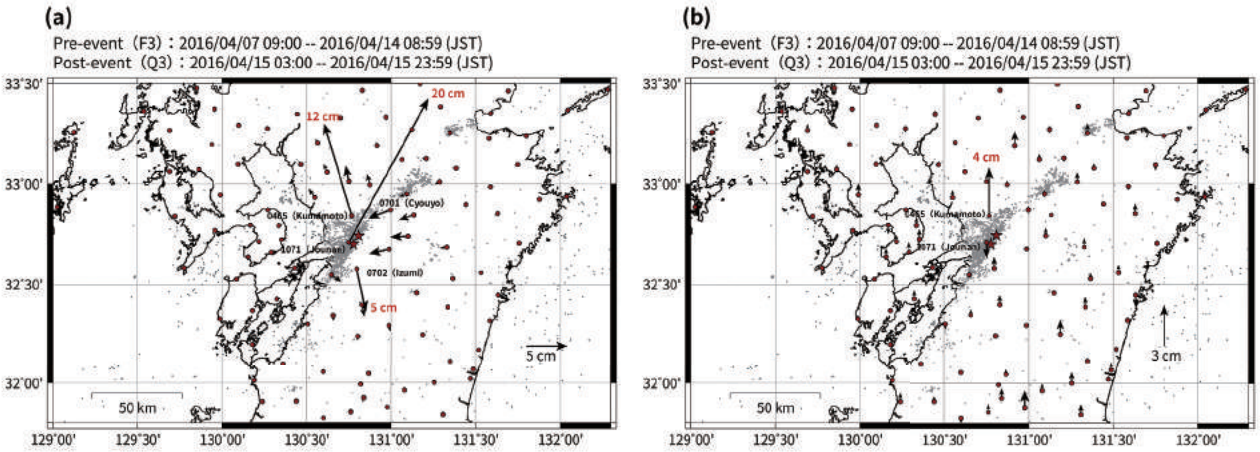

Fig. 2 Coseismic displacements due to the two large foreshocks (April 14 event [M 6.5] and April 15 event [M 6.4]). (a) Horizontal displacements. (b) Vertical displacements. The displacements were calculated as the differences between the mean position of F3 and Q3 solutions for the periods April 7, 09:00 to April 14, 08:59 (JST) and April 15, 03:00 to April 15, 23:59 (JST), respectively.

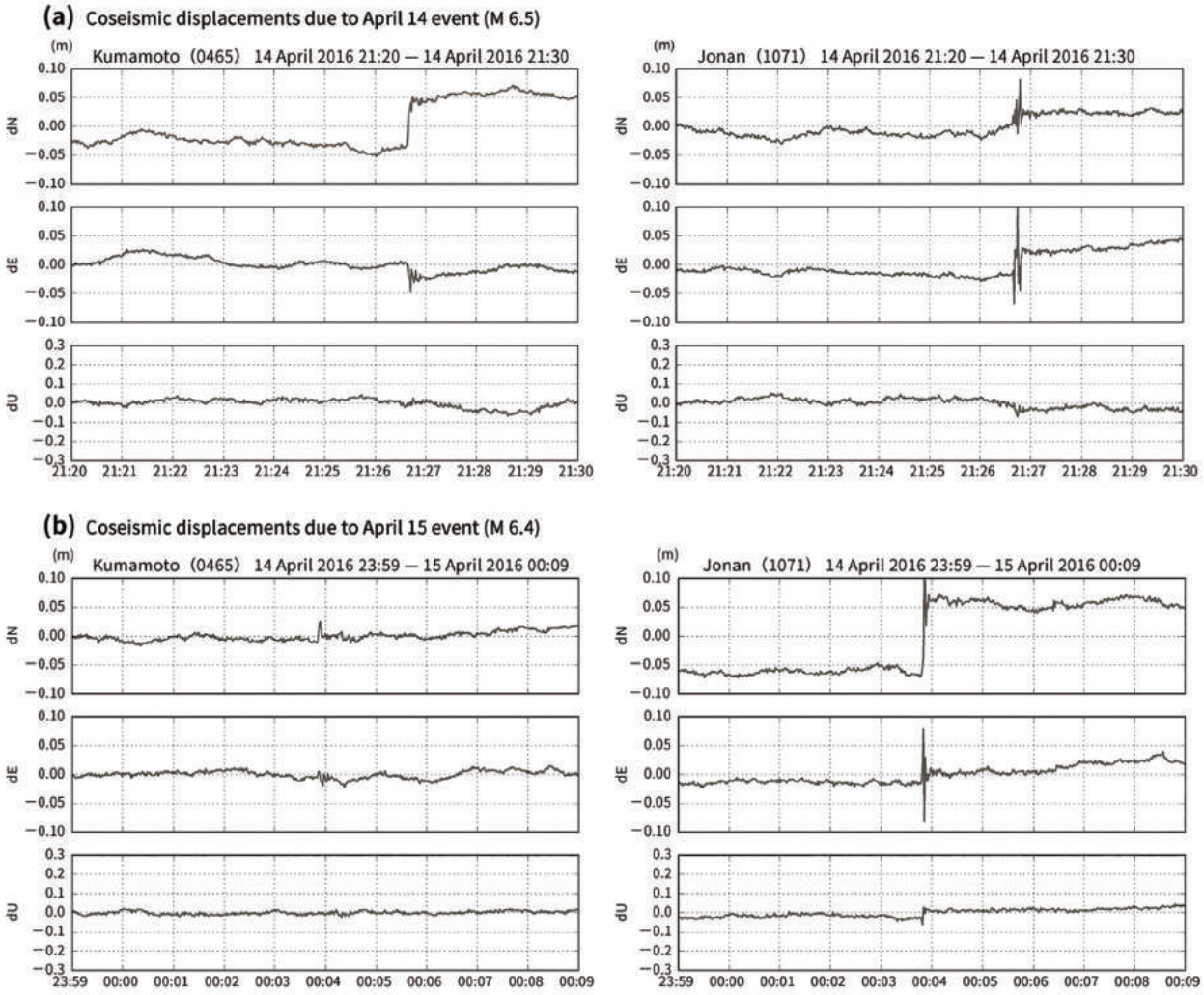

Fig. 3 Time-series of kinematic positioning from REGARD system during the (a) April 14 event (M 6.5) and (b) April 15 event (M 6.4). The time-series at site 0465 (left) and site 1071 (right) are shown.

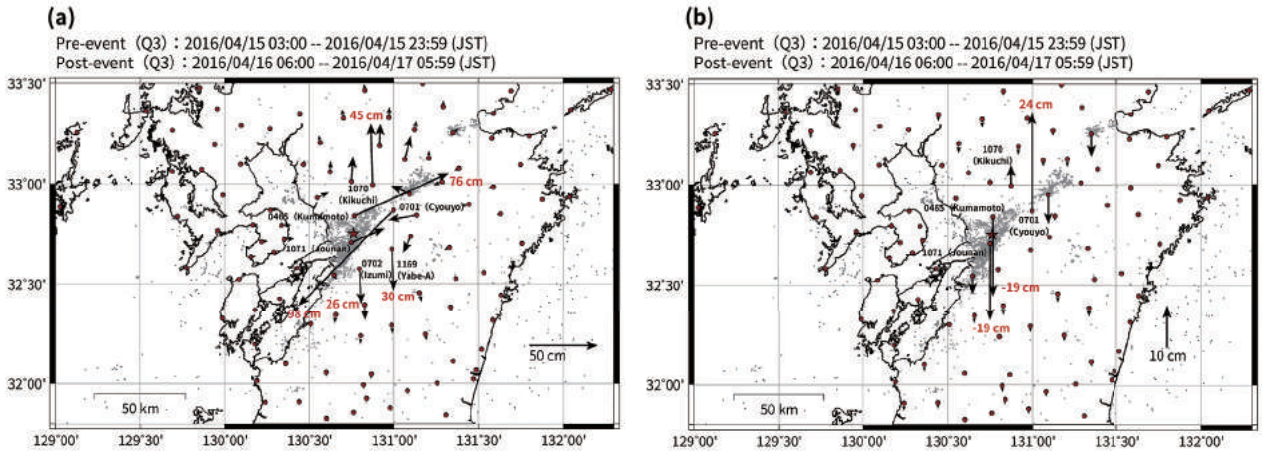

Fig. 4 Coseismic displacements caused by the mainshock (M 7.3). (a) Horizontal displacements. (b) Vertical displacements. The displacements were calculated as differences between the mean position of Q3 solutions for the periods April 15 03:00 to April 15 23:59 (JST) and April 16 06:00 to April 17 05:59 (JST), respectively.

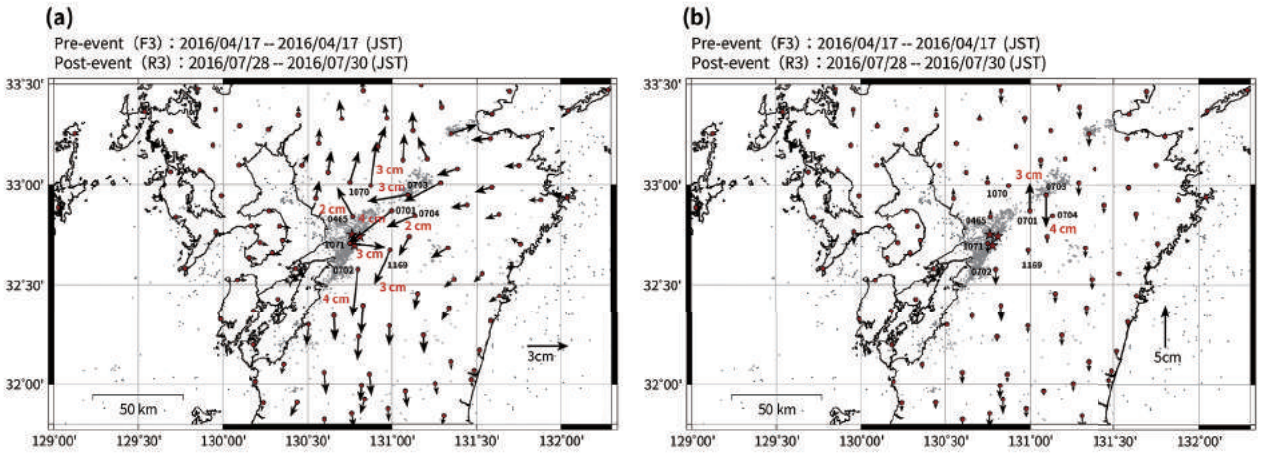

Fig. 5 Postseismic displacements over the first ~100 days following the mainshock. (a) Horizontal displacements. (b) Vertical displacements. The displacements were calculated as differences between the mean position of F3 and R3 solutions for the periods April 17 to April 17 (JST) and July 28 to July 30 (JST), respectively.

Coseismic displacements caused by each foreshock were identified using the kinematic positioning results provided by the REGARD system. For the first foreshock, the 1 Hz displacement time-series show a larger displacement at site 0465 north of the Futagawa fault (Fig. 3a), and the NW displacement of over 10 cm at 0465 was consistent with the displacement from the routine analysis. However, the horizontal displacement at 1071 was ~6 cm, clearly smaller than the displacement from the routine analysis (Fig. 2, Fig. 3a). In contrast to the first foreshock, coseismic horizontal displacement at 1071 was over 10 cm as caused by the second foreshock (Fig. 3b). This result can be explained that the two large foreshocks ruptured different portions of the fault; the first foreshock occurred at the northern part of the Hinagu fault, then the second foreshock ruptured just south of the first rupture. For more detail, see Kobayashi (2016), Kawamoto et al. (2016), and Yarai et al. (2016).

3. Coseismic Deformation Caused by the Mainshock (*M* 7.3)

The mainshock (*M* 7.3) occurred on April 16, 2016 at 01:25 JST. Its epicenter was around the northern end of the Hinagu fault segment, and it was followed by aftershocks distributed along an active strike slip fault known as the Futagawa fault (Yagi et al., 2016).

The time interval between the mainshock and the April 15 event (*M* 6.4) was over a day, thus the coseismic displacements were successfully detected using the routine analysis. To reduce the effect of early post-seismic deformation, the Q3 solution for a day was averaged to estimate post event coordinates, instead of using averaging period of 7 days used for Fig. 2. Therefore, the extracted coseismic deformation might be noisier than that of the two foreshocks.

Significantly large coseismic displacements up to ~ 1m were caused by the mainshock (Fig. 4). NE displacement of 76 cm and subsidence of 19 cm, and SW displacement of 98 cm and uplift of 24 cm were detected just after the mainshock at sites 0465 and 0701. Both sites are located near the Futagawa fault, especially site 0701 is located at western end of Aso Caldera, which is about 25 km away from the epicenter. The deformation field did not include pure symmetric displacements: site 1070 north of the fault showed larger displacement of 45 cm as compared to the displacement at site 1169 south of the fault.

The coseismic deformation field implies the earthquake fault may extend from the epicenter around the junction of Hinagu–Futagawa fault to the western part of Aso Caldera with ~25 km length. Furthermore, the fault plane may be north-dipping because the horizontal displacements were larger at sites on upper fault (north of fault trace). InSAR observation also shows larger deformation in the north area of the Futagawa fault segment (Miyahara et al., 2016) that is in good agreement with the GNSS observation. For more detail see Yarai et

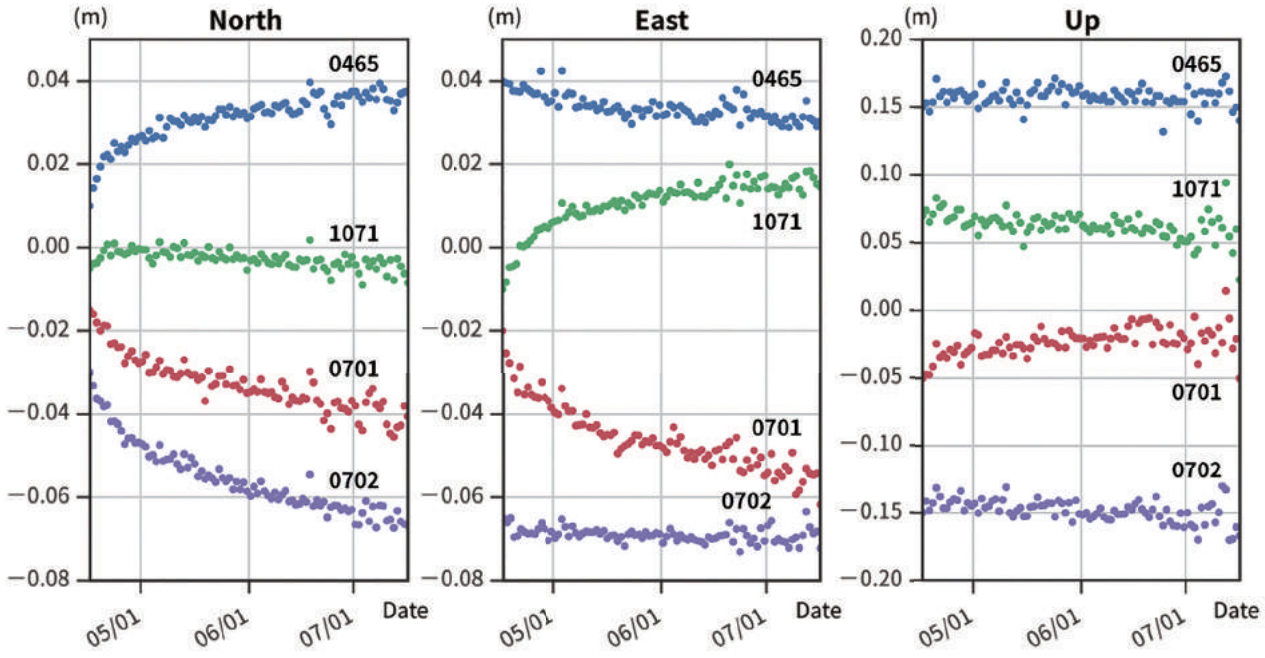

Fig. 6 Time-series of postseismic deformations at sites 0465 (blue), 1071 (green), 0701 (red), and 0702 (purple; from top to bottom). North (left), east (center), and up (right) components are shown.

al. (2016) that presents rectangular fault model inferred from the GNSS and InSAR data, showing right-lateral fault with some of north-dipping normal component.

The Japanese geodetic datum (JGD 2011; Hiyama et al. [2011]) around the Kumamoto region was largely distorted by the crustal deformation related to the 2016 Kumamoto earthquakes, thus an update of the official coordinates for the reference points (triangular stations) is planned. The distorted area was determined based on continuous GNSS observation of GEONET so that the strain is expected to be negligible compared to the accuracy of geodetic surveys. For more detail see Ootaki et al. (2016) in this special issue.

4. Postseismic Deformation after the 2016 Kumamoto Earthquake

Postseismic deformation has been widely observed around the focal area of the 2016 Kumamoto Earthquake (Fig. 5). A horizontal displacement of up to 4 cm was observed at site 0701 as of July 30, 2016. Similar to the coseismic deformation due to the mainshock, the postseismic deformation showing the deformation pattern expected from a right-lateral slip along the Futagawa fault segment, however, extends to a wider area. Time-series of the displacements show that the postseismic deformation is gradually decaying but still continuing (Fig. 6). Especially, sites 0701 and 0702 have been moving faster, and clearly have not been decayed completely. The decay curve of site 1071 is a little complicated: site 1071 has been moving towards north for ~1 week, then the direction changed toward south.

Following the numerous earthquakes, a transient slip called “afterslip” has been observed (e.g., Segall, 2010). The afterslip is expected to be an aseismic slip along strike of the coseismic rupture below the seismogenic zone with decay times ranging from months to years. Heki et al. (1997) shows the postseismic deformation after the 1994 Sanriku-Haruka-Oki earthquake can be explained by afterslip for about a year. Another possible mechanism is visco elastic relaxation, however, it has relatively long decay time (e.g. Ohzono et al., 2012), and should be dominant at this time. The fact that postseismic deformation following the Kumamoto earthquakes occurs over a wide area could be explained by afterslip on deeper part of the coseismic rupture, however, a more detailed investigation is left for future work.

5. Summary and Concluding Remarks

GNSS observation using GEONET provided information on coseismic deformations caused by the 2016 Kumamoto Earthquake sequence. Coseismic displacement over 10 cm was detected after the foreshocks, and individual displacements were successfully separated using 1 Hz kinematic solutions with the REGARD system. Horizontal displacement up to ~ 1m was caused by the mainshock. Moreover, this large earthquake caused significant postseismic deformation of a few centimeters which was detected over a wide area. Although the mechanism of postseismic deformation is not presented in this paper, it seems to be caused by afterslip on deeper extent of the coseismic fault plane. The distorted part of the Japanese geodetic data will be updated according to the displacements observed by GEONET thus enabling quick response. In addition to scientific contributions, another important purpose of GEONET is to maintain the geodetic frame in Japan.

GEONET is a very important infrastructure to monitor crustal deformation all over Japan. We will make effort to continue a stable observation by GEONET.

Acknowledgements

The authors thank the Japan Meteorological Agency (JMA) for provideng the earthquake catalogue. Figures were drawn using Generic Mapping Tools (Wessel and Smith, 1998) and matplotlib (Hunter, 2007).

References

Headquarters for Earthquake Research Promotion (2013): Evaluation of Active Faults to Date. http://jishin.go.jp/main/chousa/katsudansou_pdf/93_futagawa_hinagu_2.pdf (accessed August 3, 2016). (in Japanese).

Headquarters for Earthquake Research Promotion (2016): Evaluation of the 2016 Kumamoto Earthquakes, http://www.jishin.go.jp/main/chousa/16may_kumamoto/index-e.htm (accessed August 3, 2016).

Heki, K., S. Miyazaki and H. Tsuji (1997): Silent Fault Slip Following an Interplate Thrust Earthquake at the Japan Trench, Nature, 386, 595–598.

Hiyama, Y., A. Yamagiwa, T. Kawahara, M. Iwata, Y. Fukuzaki, Y. Shouji, Y. Sato, T. Yutsudo, T. Sasaki, H. Shigematsu, H. Yamao, T. Inukai, M. Ohtaki, K. Kokado, S. Kurihara, I. Kimura, T. Tsutsumi, T. Yahagi, Y. Furuya, I. Kageyama, S. Kawamoto, K. Yamaguchi, H. Tsuji and S. Matsumura (2011): Revision of Survey Results of Control Points after the 2011 Tohoku Earthquake off the Pacific Coast, Bulletin of GSI, 59, 31–42.

Hunter, JD (2007): Matplotlib: A 2D Graphics Environment, Computing In Science and Engineering, 9(3), 90–95.

Kawamoto, S., K. Miyagawa, T. Yahagi, M. Todoriki, T. Nishimura, Y. Ohta, R. Hino and S. Miura (2015): Development And Assessment Of Real-Time Fault Model Estimation Routines In The GEONET Real-Time Processing System, International Association of Geodesy Symposia 2015, doi:10.1007/1345_2015_49.

Kawamoto, S., Y. Hiyama, Y. Ohta and T. Nishimura (2016): First Result From The GEONET Real-Time Analysis System (REGARD): The Case Of The 2016 Kumamoto Earthquakes, Earth, Planets and Space 68: 190. doi: 10.1186/s40623-016-0564-4

Kobayashi, T. (2016): Earthquake Rupture Properties For Foreshocks (Mj6.5 and Mj6.4) of the 2016 Kumamoto Earthquakes, Revealed By Conventional And Multiple-Aperture Insar, submitted to the Special Issue on Earth, Planets And Space.

Matsumoto, S., S. Nakao, T. Ohkura, M. Miyazaki, H. Shimizu, Y. Abe, H. Inoue, M. Nakamoto, S. Yoshikawa and Y. Yamashita (2015): Spatial Heterogeneities In Tectonic Stress In Kyushu, Japan And Their Relation To A Major Shear Zone, Earth, Planets And Space, 67: 172. doi:10.1186/s40623-015-0342-8.

Miyahara, B., Y. Miura, Y. Kakiage, H. Ueshiba, M. Honda, H. Nakai, Y. Morishita, T. Kobayashi, H. Yarai and S. Fujiwara (2016): Detection of Ground Surface Deformation Caused by the 2016 Kumamoto Earthquake by InSAR using ALOS-2 Data, Bulletin of the Geospatial Information Authority of Japan, 64, 21-26.

Ohzono, M., Y. Ohta, T. Iinuma, S. Miura and J. Muto (2012): Geodetic Evidence Of Viscoelastic Relaxation After The 2008 Iwate-Miyagi Nairiku Earthquake, Earth, Planets and Space, 64, 759–764.

Ootaki, O., T. Inoue, T. Yamashita, S. Omori, K. Yamaguchi, H. Shirai, A. Suzuki and K. Mikihara

(2016): Revision of the Results of Control Points after the 2016 Kumamoto Earthquakes, Journal of the Geospatial Information Authority of Japan, 128, 177-187. (in Japanese)

Saiga, A., S. Matsumoto, K. Uehira, T. Matsushima and H. Shimizu (2010): Velocity Structure In The Crust Beneath The Kyushu Area, Earth, Planets And Space, 62, 449–462.

Segall, P. (2010): Earthquake and Volcano Deformation, Princeton University Press, 456 pp.

Wessel, P., WHF Smith (1998): New, Improved Version Of Generic Mapping Tools Released, Eos Trans. AGU, 79(47): 579.

Yagi, Y., R. Okuwaki, B. Enescu, A. Kasahara, A. Miyakawa and M. Otsubo (2016): Rupture Process Of The 2016 Kumamoto Earthquakes In Relation To The Thermal Structure Around Aso Volcano, Earth, Planets And Space 68: 118. doi:10.1186/s40623-016-0492-3.

Yamagiwa, A., Y. Hatanaka, T. Yutsudo, B. Miyahara (2006): Real-Time Capability Of GEONET System And Its Application To Crust Monitoring, Bulletin of the GSI, 53, 27–33.

Yarai H., T. Kobayashi, S. Kawamoto, Y. Morishita, S. Fujiwara, H. Munekane, Y. Hiyama, K. Yamaguchi, A. Suzuki, S. Abe, B. Miyahara, Y. Miura, Y. Kakiage and H. Ueshiba (2016): Overview Of Crustal Deformation Associated With The 2016 Kumamoto Earthquakes, submitted to the special issue on Earth, Planets and Space.